Theoretical and Mathematical Physics, **195**(2): 718–728 (2018)

SPECTRAL GAP OF THE ANTIFERROMAGNETIC LIPKIN–MESHKOV–GLICK MODEL

R. G. Unanyan*

We study the spectral property of the supersymmetric (SUSY) antiferromagnetic Lipkin–Meshkov–Glick (LMG) model with an even number of spins and explicitly construct the supercharges of the model. Using the exact form of the SUSY ground state, we introduce simple trial variational states for the first excited states. We show numerically that they provide a relatively accurate upper bound for the spectral gap (the energy difference between the ground state and first excited states) in all parameter ranges, but because it is an upper bound, it does not allow rigorously determining whether the model is gapped or gapless. To answer this question, we obtain a nontrivial lower bound for the spectral gap and thus show that the antiferromagnetic SUSY LMG model is gapped for any even number of spins.

Keywords: integrable model, Lipkin–Meshkov–Glick model, many-body system, spectral gap

DOI: 10.1134/S0040577918050070

1. Introduction

About fifty years ago, Lipkin, Meshkov, and Glick (LMG) introduced an exactly solvable model of interacting fermions in nuclear physics [1]. This model subsequently found widespread use in not only nuclear physics but also a variety of other fields of physics, such as Bose–Einstein condensates [2], ion traps [3], and cavities [4]. The LMG Hamiltonian is

$$H = \xi(\chi_1^2 J_x^2 + \chi_2^2 J_y^2 + \lambda\chi_1\chi_2 J_z), \qquad J_i = \frac{1}{2}\sum_{n=1}^{N}\sigma_i^{(n)}, \quad i = x, y, z, \tag{1}$$

where J_i are the familiar angular momentum operators, $\sigma_i^{(n)}$ are the Pauli matrices, and N is the total number of spins. Here, we focus on the manifold with the maximum angular momentum $J = N/2$, where N is an even integer. Hence, the Hilbert space has dimension $2J+1$. The parameters χ_1, χ_2, and λ are assumed to be positive constants. At the point where $\chi_2 = 0$, the ground state of Hamiltonian (1) is either ferromagnetic or antiferromagnetic depending on the sign of ξ. Here, we discuss the antiferromagnetic case ($\xi > 0$) and without loss of generality set $\xi = 1$. We note that the rotation $\exp(i\pi J_x/2)$ transforms Hamiltonian (1) into the form $\chi_1^2 J_y^2 + \chi_2^2 J_x^2 + \lambda\chi_1\chi_2 J_z$, and we can therefore assume that $\chi_1 \geq \chi_2$.

As noted in [3], the spectrum of model (1) at $\lambda = 1$ has a two-fold degeneracy in the excitation spectrum and a nondegenerate ground state with zero energy. These observations manifest the presence

*Department of Physics, Kaiserslautern University of Technology, Kaiserslautern, Germany, e-mail: unanyan@physik.uni-kl.de.

Prepared from an English manuscript submitted by the author; for the Russian version, see *Teoreticheskaya i Matematicheskaya Fizika*, Vol. 195, No. 2, pp. 256–268, May, 2018. Original article submitted June 2, 2017; revised July 26, 2017.

of a supersymmetry (SUSY) in the system. So far as we know, there is still no mathematical proof that Hamiltonian (1) is supersymmetric and a nonzero spectral gap (the energy difference between the ground state and first excited states) exists in the spectrum for $\lambda = 1$. Our aim here is to present a detailed proof of these facts. A good introduction to SUSY theory can be found, for example, in [5].

First, we show that the LMG model at $\lambda = 1$ is indeed supersymmetric by constructing the supercharges Q_1 and Q_2

$$H = Q_1^2 = Q_2^2, \tag{2}$$

and we show that they anticommute, i.e.,

$$\{Q_1, Q_2\} = 0. \tag{3}$$

One consequence of this result is that it automatically yields the two-fold degeneracy of excited states [5]. Analogous results were obtained using elaborate approximations in the framework of the WKB method [6].

Second, we obtain upper and lower bounds for the spectral gap ΔE, i.e., the first excited state energy (because the ground state energy is zero) of Hamiltonian (1). We show that knowing the ground state allows obtaining a reasonable upper bound for the spectral gap using relatively simple variational states. The obtained bounds increase as the system size increases. As a rule, the variational estimates usually agree well with exact eigenvalues of a Hamiltonian. Hence, it is natural to expect that the true spectral gap of the antiferromagnetic SUSY LMG model also increases as J increases. We confirm this numerically and, moreover, provide a nontrivial lower bound for the first excited state energy. We thus rigorously prove that system (1) at the SUSY point is indeed gapped for any integer value of J.

2. SUSY in the LMG model

The analysis of the spectrum of Hamiltonian (1) can be greatly simplified by introducing a new set of variables Ω_0 and γ:

$$\chi_1 = \Omega_0 \cosh\gamma, \qquad \chi_2 = \Omega_0 \sinh\gamma, \qquad \Omega_0^2 = \chi_1^2 - \chi_2^2, \qquad \tanh\gamma = \frac{\chi_2}{\chi_1}. \tag{4}$$

Hamiltonian (1) can be factored using the identity

$$\exp(-\gamma J_z) J_x \exp(\gamma J_z) = J_x \cosh\gamma - i J_y \sinh\gamma \tag{5}$$

for a hyperbolic rotation around the z axis with the parameter γ as

$$\begin{aligned} H &= \Omega_0^2 (J_x \cosh\gamma + i J_y \sinh\gamma)(J_x \cosh\gamma - i J_y \sinh\gamma) = \\ &= \Omega_0^2 \exp(-\gamma J_z)\, J_x \exp(2\gamma J_z)\, J_x \exp(-\gamma J_z). \end{aligned} \tag{6}$$

It is easy to see from this equation that for arbitrary values of γ, all eigenvalues of Hamiltonian (6) are nonnegative: $E \geq 0$. We note that the unitary transformation $\exp(i\pi J_x)$ changes the operator $J_z \to -J_z$ and the spectrum of the Hamiltonian is therefore symmetric under $\gamma \to -\gamma$. It hence suffices to restrict ourself to considering positive γ. One purpose here is to show that LMG model (1) is supersymmetric at $\lambda = 1$. Instead of defining the Q_1 and Q_2 operators in terms of fermionic operators, we give their block-matrix representation in two invariant subspaces labeled by the "fermionic" number operator $F = (\mathbb{1} + \exp(i\pi(J_z + J)))/2$. The operator F has two distinct eigenvalues 0 and 1 with the respective multiplicities $J + 1$ and J.

It is easy to see that the matrices

$$Q_1 = \begin{pmatrix} \underbrace{0}_{(J+1)\times(J+1)} & \underbrace{B}_{(J+1)\times(J)} \\ \underbrace{B^\dagger}_{(J)\times(J+1)} & \underbrace{0}_{J\times J} \end{pmatrix}, \qquad Q_2 = \begin{pmatrix} \underbrace{0}_{(J+1)\times(J+1)} & \underbrace{-iB}_{(J+1)\times(J)} \\ \underbrace{iB^\dagger}_{(J)\times(J+1)} & \underbrace{0}_{J\times J} \end{pmatrix}, \tag{7}$$

where

$$\begin{gathered} B_{m_1,m_2} = \Omega_0 \langle m_1 | J_x \cosh\gamma + iJ_y \sinh\gamma | m_2\rangle, \\ m_1 = J, J-2, \ldots, -J, \qquad m_2 = J-1, J-3, \ldots, -J+1, \end{gathered} \tag{8}$$

satisfy anticommutation relation (3). The symbol $\underbrace{}_{(M)\times(N)}$ denotes an $M\times N$ matrix. We show that relations (2) also hold for matrices (7). Indeed,

$$Q_1^2 = Q_1^2 = \begin{pmatrix} \underbrace{BB^\dagger}_{(J+1)\times(J+1)} & \underbrace{0}_{(J+1)\times(J)} \\ \underbrace{0}_{(J)\times(J+1)} & \underbrace{B^\dagger B}_{J\times J} \end{pmatrix},$$

and according to (8), we have

$$(BB^\dagger)_{m_1,n_1} = \Omega_0^2 \sum_{m_2=J-1,J-3,\ldots,-J+1} \langle m_1 | J_x \cosh\gamma + iJ_y \sinh\gamma | m_2\rangle \langle m_2 | J_x \cosh\gamma - iJ_y \sinh\gamma | n_1\rangle$$

for $m_1, n_1 = J, J-2, \ldots, -J$. Inserting the resolution of identity

$$\sum_{m=J-1,J-3,\ldots,-J+1} |m\rangle\langle m| = \mathbb{1} - \sum_{m=J,J-2,\ldots,-J} |m\rangle\langle m| \tag{9}$$

into the sum, we can write

$$\begin{aligned} (BB^\dagger)_{m_1,n_1} &= \Omega_0^2 \langle m_1 | J_x^2 \cosh^2\gamma + J_y^2 \sinh^2\gamma + J_z \sinh\gamma\cosh\gamma | n_1\rangle - \\ &\quad - \Omega_0^2 \sum_{m=J,J-2,\ldots,-J} \langle m_1 | J_x \cosh\gamma + iJ_y \sinh\gamma | m\rangle \langle m | J_x \cosh\gamma - iJ_y \sinh\gamma | n_1\rangle = \\ &= \Omega_0^2 \langle m_1 | J_x^2 \cosh^2\gamma + J_y^2 \sinh^2\gamma + J_z \sinh\gamma\cosh\gamma | n_1\rangle. \end{aligned}$$

In the last equality, we use the fact that $\langle m_1 | J_x \cosh\gamma + iJ_y \sinh\gamma | m\rangle = 0$ for any m_1 and m in the set $\{J, J-2, \ldots, -J\}$. Analogously, for any m_2 and n_2 in the set $\{J-1, J-3, \ldots, -J+1\}$, we have

$$(B^\dagger B)_{m_2,n_2} = \Omega_0^2 \langle m_2 | J_x^2 \cosh^2\gamma + J_y^2 \sinh^2\gamma + J_z \sinh\gamma\cosh\gamma | n_2\rangle.$$

Combining these two expressions, we can partition Hamiltonian (1) in the eigenbasis of F into the block-diagonal form

$$H = \Omega_0^2 \begin{pmatrix} \underbrace{J_x^2 \cosh^2\gamma + J_y^2 \sinh^2\gamma + J_z \sinh\gamma\cosh\gamma}_{(J+1)\times(J+1)} & \underbrace{0}_{(J+1)\times(J)} \\ \underbrace{0}_{(J)\times(J+1)} & \underbrace{J_x^2 \cosh^2\gamma + J_y^2 \sinh^2\gamma + J_z \sinh\gamma\cosh\gamma}_{J\times J} \end{pmatrix}.$$

We have thus proved that Hamiltonian (1) is supersymmetric for $\lambda = 1$.

Factored form (6) allows writing the normalized ground state in the explicit form

$$|\Psi_{\rm g}\rangle = \frac{1}{\sqrt{P_J(\cosh 2\gamma)}} \exp(\gamma J_z)|m_x\rangle \quad \text{for } m_x = 0, \tag{10}$$

where $P_J(x)$ are Legendre polynomials and $|m_i\rangle = |m\rangle$, $i = x, y, z$, denotes the eigenvector of J_i associated with the magnetic quantum number m. But for the excited states, no further information can be obtained from SUSY algebra (2), (3) other than that they are two-fold degenerate. Nevertheless, as we show below, the explicit form of the ground state can be used to find an accurate upper bound for the spectral gap.

3. Upper bounds for the spectral gap

If the ground state is known, then an upper bound for the spectral gap ΔE can be found from the inequality [7]

$$\Delta E \leq \frac{\langle\Phi|H|\Phi\rangle}{1 - |\langle\Phi|\Phi_{\rm g}\rangle|^2}, \tag{11}$$

where $|\Phi_{\rm g}\rangle$ and $|\Phi\rangle$ are the respective normalized ground and trial wave functions.

For calculation purposes, it is convenient to transform Hamiltonian (6) into a unitarily equivalent form:

$$H = \Omega_0^2(J_z^2 \, \cosh^2\gamma + J_y^2 \, \sinh^2\gamma - J_x \sinh\gamma\cosh\gamma) =$$

$$= \Omega_0^2 \exp(-\gamma J_x)\, J_z \exp(2\gamma J_x)\, J_z \exp(-\gamma J_x). \tag{12}$$

Guided by our physical intuition, we choose the trial state vector

$$|\Phi_0\rangle = \frac{\exp(-\gamma J_x)}{\sqrt{\langle +|\exp(-2\gamma J_x)|+\rangle}}|+\rangle, \tag{13}$$

where

$$|+\rangle = \frac{1}{\sqrt{2}}(|m_z = 1\rangle + |m_z = -1\rangle). \tag{14}$$

The following circumstances dictate this choice. First, for small and large γ, it coincides with the first excited state of Hamiltonian (12). Indeed, it is straightforward to show that the Hamiltonian for these two limit cases takes the simple form

$$H \approx \begin{cases} \Omega_0^2 J_z^2, & \gamma \to 0, \\ \Omega_0^2 \dfrac{e^{2\gamma}}{4}(J(J+1) - J_x(J_x+1)), & \gamma \to \infty. \end{cases} \tag{15}$$

It is clear from (13) that for large $\delta = \gamma J \gg 1$, the state $|\Phi_0\rangle$ coincides with the first excited state $|m_x\rangle = |-J\,\rangle$ of (15). This is because the operator $\exp(-\gamma J_x)$ for large δ projects any state onto $|-J\rangle$. On the other hand, for small δ, the state $|\Phi_0\rangle$ coincides with $|+\rangle$, which is obviously a possible eigenstate for the first excited state of (15). Second, vector (13) is orthogonal to the ground state vector

$$|\Phi_{\rm g}\rangle = \frac{1}{\sqrt{P_J(\cosh 2\gamma)}} \exp(\gamma J_x)|m_z\rangle \quad \text{for } m_z = 0, \tag{16}$$

although this property of trial states is inessential for estimating the spectral gap by inequality (11). The orthogonality between states (13) and (16) allows calculating ΔE more simply.

We note that the state

$$|\Phi_{\rm v}(\eta)\rangle \sim (\exp(-\gamma J_x) + \eta)|+\rangle \tag{17}$$

is also a suitable trial state vector for arbitrary values of η. By comparison with numerical simulations below, we show that a proper choice of the parameter η in states (17) and (13) yields almost the same upper bound for ΔE.

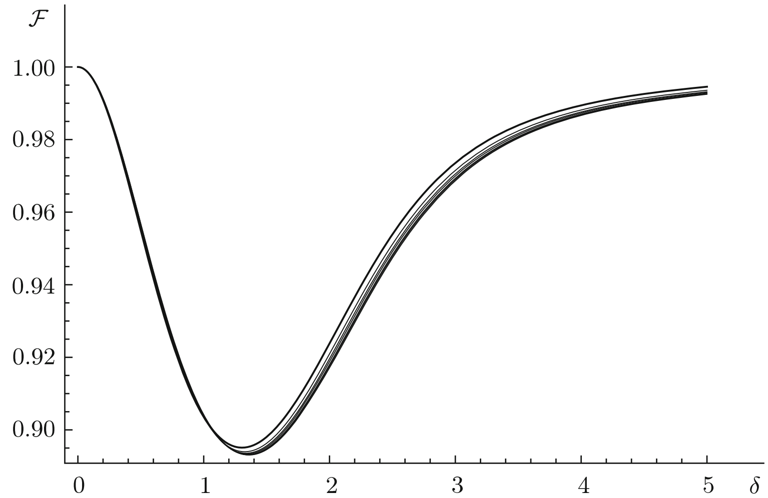

Fig. 1. Fidelity as a function of $\delta = \gamma J$ for different values of $J = 10, \dots, 100$ (from top down as J increases): for large J, the curves become virtually indistinguishable.

3.1. Fidelity. To quantify the exactness of trial vector (13), we calculate the fidelity $\mathcal{F}$ depending on the parameter $\delta = \gamma J$ for different values of J. The fidelity is simply the modulus of the overlap between state (13) and the exact (numerical) excited state of Hamiltonian (12):

$$\mathcal{F} = |\langle \Phi_{\text{exact}} | \Phi_0 \rangle|. \tag{18}$$

As we saw, the first excited states are degenerate because of the SUSY. Maximizing the fidelity over all possible superposition states with the same energy, we show the fidelity $\mathcal{F}$ in Fig. 1 as a function of $\delta = \gamma J$ for different values of J (J ranges from 10 to 100). The fidelity is generally high ($\mathcal{F} \gtrsim 0.89$) with a region of lower fidelity near $\delta = \gamma J \sim 1$. The exactness of (13) for large and small δ is unsurprising: we chose state (13) to do this. But it is surprising to us that the trial state also describes an exact excited state with high fidelity for intermediate values of δ, where perturbation theories are inapplicable.

We now return to the discussion of the spectral gap in our system.

3.2. Variational upper bound for the gap. Having discussed the exactness of our trial vector (13), we now compare the expectation value of the energy $\Delta E_0 = \langle \Phi_0 | H | \Phi_0 \rangle$ of state (13) to the exact excited state energy by calculating the ratio $\Delta E / \Delta E_0$. To express $\langle \Phi_0 | H | \Phi_0 \rangle$ in suitable form, we use the identity

$$[\exp(-\gamma J_y)]_{m,m'} = d^J_{m',m}(i\gamma), \tag{19}$$

where $d^J_{m',m}(x)$ is the Wigner rotation matrix, familiar from quantum mechanics [8]. After a lengthy but straightforward calculation, we eventually obtain the expression

$$\Delta E_0 = \Omega_0^2 \Bigg(\cosh 2\gamma + \\ + (J+2) \frac{P^{1,3}_{J-2}(\cosh 2\gamma) \sinh\gamma \, \cosh^3\gamma + P^{-3,-1}_{J+2}(\cosh 2\gamma) \, \sinh^{-3}\gamma \cosh^{-1}\gamma}{P^{0,2}_{J-1}(\cosh 2\gamma) \, \cosh^2\gamma + P^{2,0}_{J-1}(\cosh 2\gamma) \, \sinh^2\gamma} \sinh 2\gamma \Bigg), \tag{20}$$

where $P^{\alpha,\beta}_n(x)$ are Jacobi polynomials [9].

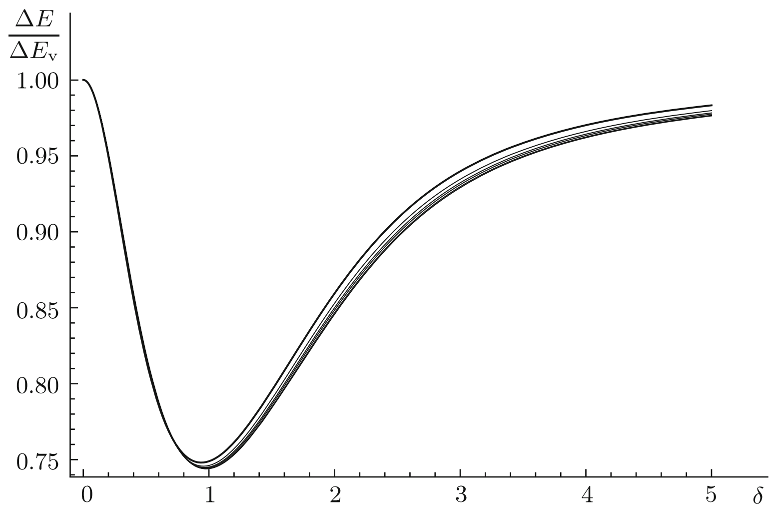

Fig. 2. Energy of first excited states as a function of $\delta = \gamma J$ with respect to variational bound (20) for different $J = 1, \ldots, 100$.

To illustrate that the upper bound ΔE_0 can be regarded as an accurate estimate of the gap, we have numerically calculated the first excited state energy ΔE of the Hamiltonian. In Fig. 2, we show $\Delta E/\Delta E_0$ as a function of δ for different values of J.

As can be seen from Fig. 2, the behavior of $\Delta E/\Delta E_0$ is very similar to the fidelity $\mathcal{F}$. For sufficiently large values of J and $\gamma \neq 0$, we can easily obtain a simple expression for ΔE_0. Using the asymptotic form of the Jacobi polynomials for large J [9]

$$P_J^{\alpha,\beta}(x) \approx \frac{(x^2-1)^{-1/4}}{\sqrt{2\pi J}}\left[x + (x^2-1)^{1/2}\right]^{J+1/2}(x-1)^{-\alpha/2}(x+1)^{-\beta/2}\left[(x+1)^{1/2} + (x-1)^{1/2}\right]^{\alpha+\beta},$$

where $x > 1$, we obtain the simple expression

$$\Delta E_0 \approx \Omega_0^2(\cosh 2\gamma + J \sinh 2\gamma). \tag{21}$$

We can hence see that for all $\gamma > 0$, ΔE_0 increases linearly as $J \gg 1$ increases. A better result for ΔE at intermediate values of δ can be obtained with the state $|+\rangle$. Substituting the state vector $|+\rangle$ in formula (11), we obtain

$$\Delta E_+ = \frac{\langle +|H|+\rangle}{1 - |\langle +|\Phi_{\rm g}\rangle|^2} = \Omega_0^2\,\frac{\cosh^2\gamma + \frac{(J+2)(J-1)}{4}\sinh^2\gamma}{1 - \frac{2J}{J+1}\frac{P_J^{1,-1}(\cosh\gamma)}{P_J(\cosh 2\gamma)}}. \tag{22}$$

Combining this expression with (20), we can derive an upper bound

$$\Delta E \leq \Omega_0^2 \min[\Delta E_0, \Delta E_+]. \tag{23}$$

For a state composed of $|\Phi_0\rangle$ and $|+\rangle$ states, i.e., state (17), the minimum with respect to η of the energy

$$\Delta E_{\rm v}(\eta) = \frac{\langle \Phi_{\rm v}(\eta)|H|\Phi_{\rm v}(\eta)\rangle}{\langle \Phi_{\rm v}(\eta)|\Phi_{\rm v}(\eta)\rangle - |\langle \Phi_{\rm v}(\eta)|\Phi_{\rm g}\rangle|^2} \tag{24}$$

would be better than (23). We do not explicitly give this lengthy optimal bound but instead present Fig. 3, where we show $\min_\eta \Delta E_{\rm v}(\eta)/\Delta E$ (see Fig. 3a) and $\Delta E/\min[\Delta E_0, \Delta E_+]$ (see Fig. 3b) as functions of δ.

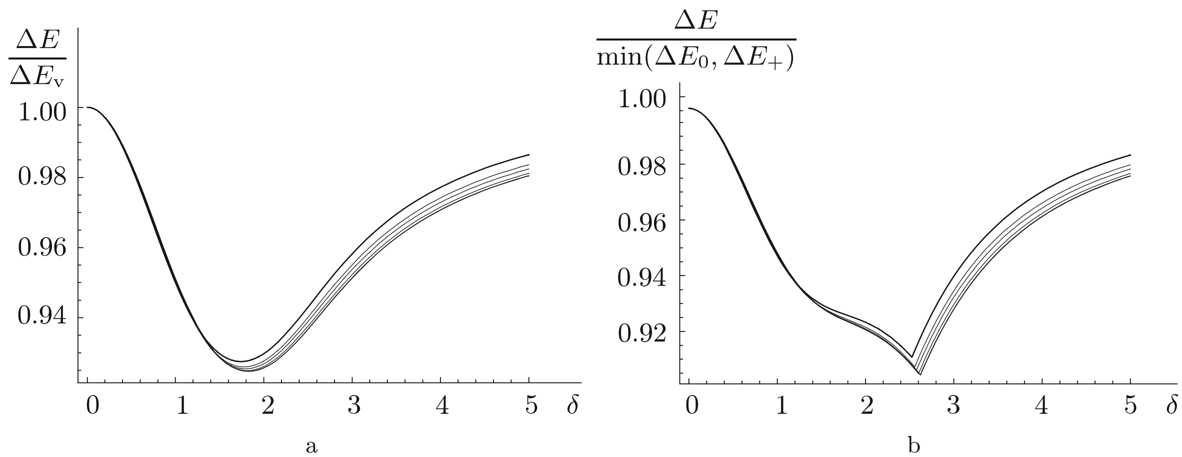

Fig. 3. Energy of first excited states as a function of $\delta = \gamma J$ with respect to the variational bounds obtained by minimizing (a) $\Delta E_v(\eta)$ and (b) $\min(\Delta E_0, \Delta E_+)$ for different $J = 1, \ldots, 100$.

As can be seen from Fig. 3a, variational state (17), which depends on the single parameter η, accurately recovers the true excited state energy within 0.8%. The accuracy of the relatively simple upper bound (23) (see Fig. 3b) is a few percent less than optimal bound (24) given by (17). It is a remarkable result considering the simplicity of the trial function used. We have thus seen that the variational upper bounds for the gap quantitatively agree well with exact numerical results (for J up 100). But these observations do not provide a rigorous proof that the system is indeed gapped. Therefore, the problem is to obtain a nontrivial lower bound for ΔE. We turn our attention to this issue.

4. Lower bound for the spectral gap

We now turn to the problem of obtaining a nontrivial lower bound for the gap by choosing a suitable form of the Hamiltonian. For this, we need some facts from matrix theory. For notational simplicity in this section, we $\lambda_n(X)$ $(n = 1, 2, \ldots, M)$ denote the eigenvalues of an $M \times M$ Hermitian matrix X in increasing order, i.e., $\lambda_1(X) \geq \lambda_2(X) \geq \cdots \geq \lambda_M(X)$.

A lower bound for the spectral gap can be obtained using the Weyl theorem [10], which is stated as follows. Let X, Y, and $Z = X + Y$ be $M \times M$ Hermitian matrices. Then

$$\lambda_{i+j-1}(Z) \leq \lambda_i(X) + \lambda_j(Y) \quad \text{for } i + j - 1 \leq M \tag{25}$$

or, equivalently,

$$\lambda_k(Z) \geq \lambda_i(X) + \lambda_j(Y) \quad \text{for } i + j = M + k. \tag{26}$$

To apply the Weyl theorem, we split Hamiltonian (12) into two parts:

$$H = H_X + \Omega_0^2 J_z^2, \tag{27}$$

where

$$H_X = \Omega_0^2\big((J_z^2 + J_y^2)\sinh^2\gamma - J_x \sinh\gamma\cosh\gamma\big) = \Omega_0^2\big((J(J+1) - J_x^2)\sinh^2\gamma - J_x \sinh\gamma\cosh\gamma\big).$$

In the second equality, we use the identity $J_z^2 + J_y^2 + J_x^2 = J(J+1)$. Using inequality (26) and recalling the SUSY property of our Hamiltonian for the spectral gap, i.e., $\Delta E = \lambda_{2J}(H) = \lambda_{2J-1}(H)$, we obtain

$$\frac{\Delta E}{\Omega_0^2} \geq \lambda_i\big[\big(J(J+1) - J_x^2\big)\sinh^2\gamma - J_x \sinh\gamma\cosh\gamma\big] + \lambda_j(J_z^2), \qquad i + j = 4J. \tag{28}$$

It is easy to verify directly that the possible pairs of (i, j) are $(2J+1, 2J-1)$, $(2J-1, 2J+1)$, and $(2J, 2J)$. The corresponding energies are

$$(2J+1, 2J-1): \qquad \frac{E_{\rm ge}}{\Omega_0^2} = 1 - Je^{\gamma}\sinh\gamma, \tag{29}$$

$$(2J-1, 2J+1): \qquad \frac{E_{\rm eg}}{\Omega_0^2} = \min\left[Je^{\gamma}\sinh\gamma,\, (5J-4)\sinh^2\gamma - \frac{J-2}{2}\sinh 2\gamma\right], \tag{30}$$

$$(2J, 2J): \qquad \frac{E_{\rm ee}}{\Omega_0^2} = 1 + (3J-1)\sinh^2\gamma - \frac{J-1}{2}\sinh 2\gamma. \tag{31}$$

Bound (29) is trivial: it goes to negative values as $\gamma > \log(1+2/J) \approx 2/J$. For small $\gamma \ll 1/J$, bound (31) is better than (30), and it becomes negative for $1/J \lesssim \gamma \lesssim 0.3$. On the other hand, for relatively large $\gamma \gtrsim 0.2$, bound (30) is much better than (31), although it becomes negative for $\gamma \lesssim 0.2$.

Hence, based on these analyses, we obtain the inequality

$$\Delta E \geq \Omega_0^2 \min\left[Je^{\gamma}\sinh\gamma,\, (5J-4)\sinh^2\gamma - \frac{1}{2}(J-2)\sinh 2\gamma\right], \tag{32}$$

which gives a trivial bound for $\gamma \lesssim 0.2$ but a nontrivial one for large γ. Comparing (21) and (32) for large γ, we conclude that the upper and lower bounds on ΔE converge to each other. It therefore remains to find a nontrivial lower bound for intermediate values of γ.

In what follows, we show that using representation (6), we can obtain the degeneracy and a nontrivial lower bound (for arbitrary γ and integer J) for ΔE by direct calculations. It is easy to see that Hamiltonian (6) resembles the non-Hermitian Hamiltonian

$$\begin{aligned} H_{\rm n} = \exp(-\gamma J_x)\, H \exp(\gamma J_x) = \Omega_0^2 \exp(-2\gamma J_x)\, J_z \exp(2\gamma J_x)\, J_z = \\ = \Omega_0^2 (J_z^2 \cosh 2\gamma + i J_y J_z \sinh 2\gamma). \end{aligned} \tag{33}$$

We show that despite its non-Hermiticity, the spectral properties of (33) are very clear. Indeed, first, it clearly has a null state $|m_z\rangle = |0\rangle$ ($J_z|0\rangle = 0$). Second, all excited states are two-fold degenerate. To see this, we note that $H_{\rm n}$ can be represented as a block matrix

$$H_{\rm n} = \begin{pmatrix} \underbrace{H_-}_{J\times J} & \underbrace{0}_{1\times J} & \underbrace{0}_{J\times J} \\ \langle a| & 0 & \langle b| \\ \underbrace{0}_{J\times J} & \underbrace{0}_{1\times J} & \underbrace{H_+}_{J\times J} \end{pmatrix} \tag{34}$$

in the eigenbasis of J_z. The matrices H_+ and H_- are real permutation equivalent, i.e., they have the same spectrum. The transposed vectors $\langle a|$ and $\langle b|$ connect the state $|m_z\rangle = |0\rangle$ with negative and positive magnetic quantum numbers m_z.

We consider $J = 2$ as an example. The Hamiltonian $H_{\rm n}$ then has the form

$$H_{\rm n} = \Omega_0^2 \begin{pmatrix} 4\cosh 2\gamma & \sinh 2\gamma & 0 & 0 & 0 \\ -2\sinh 2\gamma & \cosh 2\gamma & 0 & 0 & 0 \\ 0 & -\frac{\sqrt{6}}{2}\sinh 2\gamma & 0 & -\frac{\sqrt{6}}{2}\sinh 2\gamma & 0 \\ 0 & 0 & 0 & \cosh 2\gamma & -2\sinh 2\gamma \\ 0 & 0 & 0 & \sinh 2\gamma & 4\cosh 2\gamma \end{pmatrix},$$

where

$$H_- = \Omega_0^2 \begin{pmatrix} 4\cosh 2\gamma & \sinh 2\gamma \\ -2\sinh 2\gamma & \cosh 2\gamma \end{pmatrix}, \qquad H_+ = \Omega_0^2 \begin{pmatrix} \cosh 2\gamma & -2\sinh 2\gamma \\ \sinh 2\gamma & 4\cosh 2\gamma \end{pmatrix},$$

and

$$\langle a| = \Omega_0^2 \Big(0, -\frac{\sqrt{6}}{2}\sinh 2\gamma\Big), \qquad \langle b| = \Omega_0^2 \Big(-\frac{\sqrt{6}}{2}\sinh 2\gamma, 0\Big).$$

It can be seen that H_+ and H_- are permutation equivalent, i.e.,

$$H_- = \begin{pmatrix} 0 & 1 \\ 1 & 0 \end{pmatrix} H_+ \begin{pmatrix} 0 & 1 \\ 1 & 0 \end{pmatrix}.$$

The elements of H_+ are

$$(H_+)_{m,m'} = \Omega_0^2 \Big(m^2 \delta_{mm'} \cosh 2\gamma + \frac{m'}{2} \sinh 2\gamma \big[\delta_{m,m'+1} \sqrt{(J-m')(J+m'+1)} - \\ - \delta_{m,m'-1} \sqrt{(J+m')(J-m'+1)} \,\big] \Big), \tag{35}$$

where $m, m' = J, J-1, \dots, 1$. The spectrum of H_{n} can be obtained from the algebraic equation

$$\lambda \det(\lambda \cdot \mathbb{1}_{J\times J} - H_+) \det(\lambda \cdot \mathbb{1}_{J\times J} - H_-) = 0. \tag{36}$$

Because H_+ and H_- have the same spectrum, the spectrum of H_{n} is doubly degenerate except the eigenstate $|m_z\rangle = |0\rangle$. Therefore, we can restrict ourself to studying the spectral properties of H_+.

We thus have directly verified that for an integer J and arbitrary γ, the spectrum of initial Hamiltonian (6) is supersymmetric. In addition, the excited spectrum of Hamiltonian (6) coincides with the spectrum H_+, i.e., the spectral gap of our model coincides with the ground state energy of H_+.

As can be seen from Eq (35), the matrix H_+ can be represented in the compact form

$$H_+ = \Omega_0^2 (j_z^2 \cosh 2\gamma + i \cdot j_y j_z \sinh 2\gamma), \tag{37}$$

where the truncated Hermitian angular momentum matrices j_z, j_y, and j_x satisfy the commutation relations

$$[j_z, j_x] = i j_y, \qquad [j_y, j_z] = i j_x, \tag{38}$$

but in contrast to the ordinary angular momentum operators, we have $[j_x, j_y] \neq i j_z$.

We next show that the Hamiltonian H_+ can be transformed into a more pleasing form. For this, we recall that j_z is a positive-definite matrix with eigenvalues $1, 2, \dots, J$, and the square root $j_z^{1/2}$ is hence well defined. Using this, we can write the matrix H_+ as $H_+ = j_z^{-1/2} h\, j_z^{1/2}$, where

$$h = \Omega_0^2 (j_z^2 \cosh 2\gamma + i \cdot j_z^{1/2} j_y j_z^{1/2} \sinh 2\gamma), \tag{39}$$

which has the same spectrum as H_+. We now state that for any γ and J, we have $\Delta E \geq \Omega_0^2 \cosh 2\gamma$. Indeed, for any eigenvalue $E(h) > 0$ of h and its corresponding normalized eigenvector $|\varphi\rangle$ we have

$$E(h) = \langle\varphi|h|\varphi\rangle = \Omega_0^2 \big(\langle\varphi|j_z^2|\varphi\rangle \cosh 2\gamma + i \langle\varphi| j_z^{1/2} j_y j_z^{1/2} |\varphi\rangle \sinh 2\gamma \big) = \\ = \Omega_0^2 \langle\varphi|j_z^2|\varphi\rangle \cosh 2\gamma \geq \Omega_0^2 \cosh 2\gamma,$$

where we use the fact that $j_z^{1/2} j_y j_z^{1/2}$ is a Hermitian matrix. In the last quality, we use the fact that the smallest eigenvalue of j_z is equal to unity. Hence, all eigenvalues of h are at finite distances from the origin greater than $\Omega_0^2 \cosh 2\gamma$, i.e., the spectral gap of antiferromagnetic SUSY LMG Hamiltonian (6) is bounded from below by $\Omega_0^2 \cosh 2\gamma$. Unlike inequality (32), this quantity does not involve J.

5. Discussion and conclusion

We have investigated the spectrum of the antiferromagnetic LMG model at the SUSY point. By explicitly constructing the supercharges, we proved that Hamiltonian (1) is supersymmetric at $\lambda = 1$. Using the explicit form of the ground state of the Hamiltonian, we introduced variational excited states that have a quite high fidelity with the exact excited state. A simple form of these states allowed finding closed expressions for upper bounds on the spectral gap. We numerically showed that the obtained upper bounds agree well with the exact spectral gap. We found simple nontrivial lower bounds for the spectral gap. We thus showed that the antiferromagnetic SUSY LMG model is gapped for any values of γ.

Although for intermediate values of γ, the obtained lower bound

$$\Delta E \geq \Omega_0^2 \max\left\{\cosh 2\gamma,\, \min\left[Je^{\gamma}\sinh\gamma,\, (5J-4)\sinh^2\gamma - \frac{J-2}{2}\sinh 2\gamma\right]\right\}$$

is not tighter than those of variational bounds, it can be used to study the low-energy physics in the LMG model, for example, for estimating the duration of adiabatic quantum processes in ionic traps [11]. This lower bound can undoubtedly be improved. We hope to return to these topics in a future publication.

Acknowledgments. The author is grateful to M. Fleischhauer for the many fruitful and stimulating discussions.

REFERENCES

1. H. J. Lipkin, N. Meshkov, and A. J. Glick, "Validity of many-body approximation methods for a solvable model: (I). Exact solutions and perturbation theory," *Nucl. Phys.*, **62**, 188–198 (1965); N. Meshkov, A. J. Glick, and H. J. Lipkin, "Validity of many-body approximation methods for a solvable model: (II). Linearization procedures," *Nucl. Phys.*, **62**, 199–210 (1965); A. J. Glick, H. J. Lipkin, and N. Meshkov, "Validity of many-body approximation methods for a solvable model: (III). Diagram summations," *Nucl. Phys.*, **62**, 211–224 (1965).
2. J. I. Cirac, M. Lewenstein, K. Mølmer, and P. Zoller, "Quantum superposition states of Bose–Einstein condensates," *Phys. Rev. A*, **57**, 1208–1218 (1998).
3. R. G. Unanyan and M. Fleischhauer, "Decoherence-free generation of many-particle entanglement by adiabatic ground-state transitions," *Phys. Rev. Lett.*, **90**, 133601 (2003); R. G. Unanyan, C. Ionescu, and M. Fleischhauer, "Many-particle entanglement in the gaped antiferromagnetic Lipkin model," *Phys. Rev. A*, **72**, 022326 (2005).
4. J. Larson, "Circuit QED scheme for the realization of the Lipkin–Meshkov–Glick model," *Europhys. Lett.*, **90**, 54001 (2010); arXiv:1004.5041v2 [quant-ph] (2010); Y.-C. Zhang, X.-F. Zhou, X. Zhou, G.-C. Guo, and Z.-W. Zhou, "Cavity-assisted single-mode and two-mode spin-squeezed states via phase-locked atom–photon coupling," *Phys. Rev. Lett.*, **118**, 083604 (2017).
5. E. Witten, "Dynamical breaking of supersymmetry," *Nucl. Phys. B*, **188**, 513–554 (1981); L. E. Gendenshtein and I. V. Krive, "Supersymmetry in quantum mechanics," *Sov. Phys. Usp.*, **28**, 645–666 (1985); F. Cooper, A. Khare, and U. Sukhatme, "Supersymmetry and quantum mechanics," *Phys. Rep.*, **267**, 267–385 (1995).
6. A. Garg, "Quenched spin tunneling and diabolical points in magnetic molecules: I. Symmetric configurations," *Phys. Rev. B*, **64**, 094413 (2001); E. Keçecioğlu and A. Garg, "$SU(2)$ instantons with boundary jumps and spin tunneling in magnetic molecules," *Phys. Rev. Lett.*, **88**, 237205 (2002).
7. C. Eckart, "The theory and calculation of screening constants," *Phys. Rev.*, **36**, 878–892 (1930).
8. L. Biedenharn and J. D. Louck, *Angular Momentum in Quantum Physics: Theory and Application* (Encycl. Math. Its Appl., Vol. 8), Addison–Wesley, Reading, Mass. (1981); D. A. Varshalovich, A. N. Moskalev, and

V. K. Kheronskii, *Quantum Theory of Angular Momentum* [in Russian], Nauka, Leningrad (1975); English transl., World Scientific, Singapore (1988).

9. G. Szegö, *Orthogonal Polynomials* (Amer. Math. Soc. Colloq. Publ., Vol. 23), Amer. Math. Soc., New York (1939).
10. H. Weyl, "Das asymptotische Verteilungsgesetz der Eigenwerte linearer partieller Differentialgleichungen (mit einer Anwendung auf die Theorie der Hohlraumstrahlung)," *Math. Ann.*, **71**, 441–479 (1912); W. Fulton, "Eigenvalues, invariant factors, highest weights, and Schubert calculus," *Bull. Amer. Math. Soc.*, n.s., **37**, 209–249 (2000).
11. R. Blatt and C. F. Roos, "Quantum simulations with trapped ions," *Nature Phys.*, **8**, 277–284 (2012).